Published OnlineFirst July 29, 2019; DOI: 10.1158/0008-5472.CAN-19-0086

Tumor Biology and Immunology

Cancer Research

Inactivation of Proprotein Convertases in T Cells Inhibits PD-1 Expression and Creates a Favorable Immune Microenvironment in Colorectal Cancer

Mercedes Tomé[1,2], Angela Pappalardo[3], Fabienne Soulet[1,2], José Javier López[4], Jone Olaizola[1,2], Yannick Leger[1,2], Marielle Dubreuil[1,2], Amandine Mouchard[1,5], Delphine Fessart[5,6], Frédéric Delom[5,6], Vincent Pitard[3], Dominique Bechade[5], Mariane Fonck[5], Juan Antonio Rosado[4], François Ghiringhelli[7], Julie Déchanet-Merville[3], Isabelle Soubeyran[5], Geraldine Siegfried[1,2], Serge Evrard[1,2,5], and Abdel-Majid Khatib[1,2]

Abstract

Proprotein convertases (PC) activate precursor proteins that play crucial roles in various cancers. In this study, we investigated whether PC enzyme activity is required for expression of the checkpoint protein programmed cell death protein 1 (PD-1) on cytotoxic T lymphocytes (CTL) in colon cancer. Although altered expression of the PC secretory pathway was observed in human colon cancers, only furin showed highly diffuse expression throughout the tumors. Inhibition of PCs in T cells using the general protein-based inhibitor α1-PDX or the pharmacologic inhibitor Decanoyl-Arg-Val-Lys-Arg-chloromethylketone repressed PD-1 and exhausted CTLs via induction of T-cell proliferation and apoptosis inhibition, which improved CTL efficacy against microsatellite instable and microsatellite stable colon cancer cells. *In vivo*, inhibition of PCs enhanced CTL infiltration in colorectal tumors and increased tumor clearance in syngeneic mice compared with immunodeficient mice. Inhibition of PCs repressed PD-1 expression by blocking proteolytic maturation of the Notch precursor, inhibiting calcium/NFAT and NF-κB signaling, and enhancing ERK activation. These findings define a key role for PCs in regulating PD-1 expression and suggest targeting PCs as an adjunct approach to colorectal tumor immunotherapy.

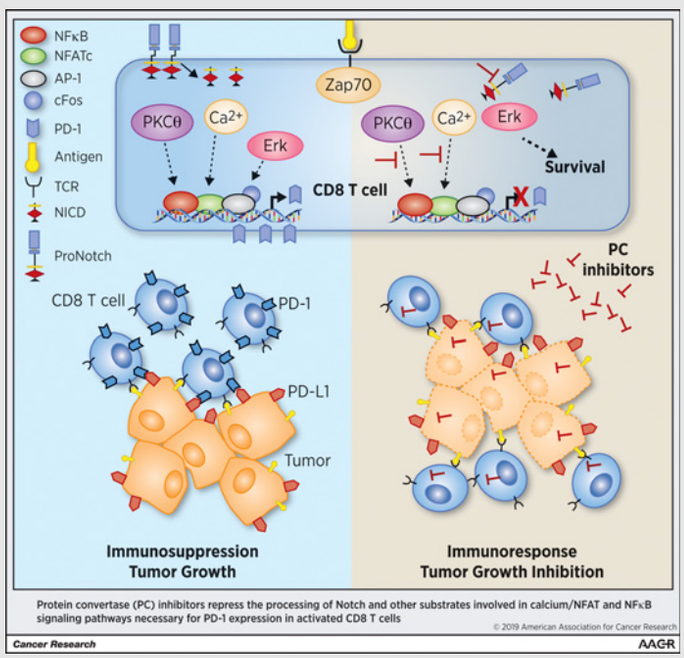

Significance: Protein convertase enzymatic activity is required for PD-1 expression on T cells, and inhibition of protein convertase improves T-cell targeting of microsatellite instable and stable colorectal cancer.

Graphical Abstract: http://cancerres.aacrjournals.org/content/canres/79/19/5008/F1.large.jpg.

[1]Université Bordeaux, Bordeaux, France. [2]INSERM UMR1029, Pessac, France. [3]ImmunoConcept, CNRS UMR 5164, University of Bordeaux, Bordeaux, France. [4]Department of Physiology, Veterinary Faculty, University of Extremadura, Caceres, Spain. [5]Institut Bergonié, Bordeaux, France. [6]INSERM U1218, ACTION, Bordeaux, France. [7]INSERM UMR1231, Dijon, France.

Note: Supplementary data for this article are available at Cancer Research Online (http://cancerres.aacrjournals.org/).

S. Evrard and A.-M. Khatib contributed equally to this article.

Corresponding Authors: Abdel-Majid Khatib, INSERM and University of Bordeaux, INSERM 1029, Bat. B2 Ouest, Allée Geoffroy St Hilaire, PESSAC 33600, France. Phone: 33-0-540002953; Fax: 33-0-540008705; E-mail: majid.khatib@u-bordeaux.fr; and Mercedes Tomé, mercedes.tome@u-bordeaux.fr

Cancer Res 2019;79:5008–21

doi: 10.1158/0008-5472.CAN-19-0086

Published OnlineFirst July 29, 2019; DOI: 10.1158/0008-5472.CAN-19-0086

Introduction

Although therapies targeting PD-1 were clinically effective in various preclinical models and patients with cancer (1, 2), the underlying mechanism involved in total remission of cancers after immunotherapy is presently unclear. In addition, the majority of patients with solid tumors, including colorectal cancers [except the microsatellite-instable (MSI) subset] are refractory to these treatments (3). The failure to respond to anti-PD-1 therapy is, in part, due to the presence of irreversibly exhausted T cells. Understanding the essential mechanism(s) involved in the lack of response to immune checkpoint blockade therapy remains a main challenge. It is well established that solid tumors evade anticancer immune control by establishing immune-privileged niches within the tumor microenvironment (TME) where intratumoral cytotoxic T lymphocytes (CTL) proliferation, viability, and activity are compromised (4). Indeed, the apparent exclusion of CTLs from colorectal cancer is associated with a poor prognosis while increased accumulation of CTLs within tumors is associated with a favorable outcome (5). Delineating the mechanisms that prevent CTL accumulation within the TME is important to understand its immunosuppressive properties and to increase the efficacy of immunotherapy (5). Upon T-cell activation, PD-1 expression is induced and regulated by the transcription factors nuclear factor of activated T-cell (NFAT), T-bet, Blimp-1, and FoxO1 (6). Various intracellular signal transduction pathways regulate expression and activation of these factors. They include tyrosine kinase, antiinflammatory signal, and mitochondrial apoptosis pathways. A wide range of proteins involved in these intracellular signal pathways require proteolytic cleavage of their protein precursors by the proprotein convertases (PC) to be biologically active (7).

PC family consists of 7 members, namely, furin, PC1, PC2, PC4, PACE4, PC5, and PC7 that convert their unprocessed substrates into functional molecules by cleaving their basic amino acid motifs (K/R)-(X) *n*-(K/R) ↓, where *n* is 0, 2, 4, or 6 and X is any amino acid (7, 8). These enzymes play an influential role not only in maintaining homeostasis but also in various pathologic conditions (7, 8). Various PCs activate proteins involved in the malignant transformation and progression including cell surface-receptors, matrix metalloproteinases, growth factors, and growth factor receptors (7–9). Altered PC levels were reported to be associated with enhanced invasion and proliferation in various tumor cells. Conversely, inhibition of PCs activity by the bioengineered inhibitor α1-PDX resulted in reduced processing of various PC substrates involved in the malignant phenotype of tumor cells (10). In a phase I and a recent phase II trial (FANG vaccine trial), an autologous tumor-based product targeting furin by shRNAi DNA was found to be beneficial in patients with advanced cancer. This FANG vaccine was safe and elicited an immune response that correlated with prolonged survival in patients (11), suggesting that furin expression/activity inhibition is an effective way of boosting antitumor response. Here, we evaluated the effect of PCs inhibition on PD-1 expression and T-cell activity. Our data indicate that PCs inactivation repressed PD-1 expression, blocked Notch cleavage and function, and increased activated T-cell proliferation, survival, and cytotoxicity against both MSI and MSS colon tumor cells. In accordance, PCs inactivation enhanced tumor-infiltrated CTLs and tumor regression *in vivo*.

Materials and Methods

Human PBMCs, T cells, and tumor samples

Patient samples were utilized in accordance with the Declaration of Helsinki, International Ethical Guidelines for Biomedical Research Involving Human Subjects (CIOMS), Belmont Report, and U.S. Common Rule. Written informed consents were obtained from all the patients and the studies were approved by Bergonié Institute and Hospital Pellegrin (France) review boards'. The medical records were de-identified. Samples were processed for RNA and histology studies. Human peripheral blood mononuclear cells (hPBMC) were isolated from healthy donors and patients with colon cancer and were directly used for RNA/protein extraction, or used for $CD8^+$ T-cell isolation. Tumor-infiltrating $CD8^+$ T cells were isolated from colon tumor samples freshly harvested following manufacturer's instructions (Miltenyi Biotec).

Cell lines

Human colon carcinoma cell lines HT29 (MSI) and HCT116 (MSS), BALB/c syngeneic colon carcinoma CT26 cell line, and human T-cell line Jurkat were purchased and authenticated by ATCC. All cell lines were passaged twice prior to storage or prior use in all described *in vitro* and *in vivo* experiments. All cell lines were determined to be free of *Mycoplasma*. Cells were cultured in DMEM or RPMI1640 complete media. The characteristics of the stably α1-PDX–expressing Jurkat cells (Jurkat-PDX) and CT26-PDX cells were described previously (12).

Mouse model

All research animals were housed in University of Bordeaux in a temperature-controlled environment. All experimental procedures were approved by the Institutional Animal Care and Use Committee (University of Bordeaux), and were conducted under the supervision of trained veterinarian. BALB/c and nude mice were inoculated subcutaneously in the right flank with 1×10^6 colon carcinoma CT26- Ø cells or CT26-PDX cells. Tumors were measured 3 times per week.

Cell infection and transfection

Lentivirus containing human NICD-pHR-EGFP plasmid and its control Ø-pHR-EGFP were kindly provided by Dr. Raúl V. Durán. Jurkat-PDX cells were infected with the control (PDX/lenti Ø) or NICD (PDX/lentiNICD) lentiviruses. NICD primers were designed to amplify only the exogenous human NICD (exoh-NICD) and not the endogenous mRNA (Supplementary Table S1). In other experiments, Jurkat cells were transfected with the EGFP-based reporter plasmid (pNFAT-TA-EGFP; kindly provided by C. Romanin, University of Linz) using DharmaFECT kb transfection reagent (Dharmacon). Cells expressing pNFAT-TA-eGFP were monitored with an epifluorescence inverted microscope (Nikon Eclipse Ti2) and Flow Cytometry for quantification. Please refer to Supplementary Information for detailed procedures.

T-cell activation

Activation of TCR signaling was performed either with phorbol myristate acetate (PMA) 100 ng/mL and Ionomycin (Io) 1 μg/mL or with plate-bound anti-CD3 (OKT3) 5 μg/mL.

Published OnlineFirst July 29, 2019; DOI: 10.1158/0008-5472.CAN-19-0086

γ-Secretase inhibitor experiments

The γ-secretase inhibitor DAPT (Sigma) was used to block Notch signaling. Jurkat-Ø cells were culture with 10 μmol/L DAPT and stimulated with PMA/Io for indicated time points. Then cells were collected for flow cytometry, immunostaining, or immunoblotting analysis.

Apoptosis assay

Jurkat-Ø and PDX cells were incubated in the presence and absence of PMA/Io for 24 and 48 hours and stained with PE-Annexin V and 7AAD using the Annexin V Apoptosis Detection Kit (BioLegend), according to the manufacturer's instructions.

Proliferation assay

Proliferation of Jurkat-Ø and PDX cells following PMA/Io activation was determined using a Countess II Automated Cell Counter (Invitrogen). Please refer to Supplementary Information for detailed procedures.

JRT3 functional assay

The Jurkat T-cell line stably expressing the human LES -γδ TCR (JRT3-LES) was incubated with the colon cancer cell line HT29 overexpressing the endothelial protein C receptor (HT29-EPCR; ref. 13). The activation of JRT3-LES cells was evaluated by the expression of CD69.

Cytometric bead array

Cytometric bead array (CBA) was used to measure the concentration of cytotoxins released by primary human $CD8^+$ T-cell populations. Please refer to Supplementary Information for detailed procedures.

Cytotoxicity assay

Susceptibility of HT29 and HCT116 to PBMC-mediated cytotoxicity was determined using a carboxyfluorescein diacetate succinimidyl ester (CFSE)-based assay. Please refer to Supplementary Information for detailed procedures.

qRT-PCR

Total RNA (1 μg) was isolated by the Nucleospin RNA Kit (Macherey-Nagel) and used for reverse transcription and qRT-PCR analysis, as described previously (8).

IHC and immunocytochemistry

Human colon cancer and its corresponding noncancer colon tissues, and syngeneic mouse tumors from CT26-Ø and CT26-PDX cells were used for IHC. IHC was performed in hPBMCs and Jurkat cells in suspension. Please refer to Supplementary Information for details on primary and secondary antibodies and procedures used.

Flow cytometry

Flow cytometry analyses were performed on single cell suspension of hPBMCs and T cells using BD Accuri C6 software, or Diva (BD Biosciences) and FlowJo 9.3.2 (TreeStar) softwares (flow cytometry facility of TBM Core).

Measurement of PC activity

The effect of PC inhibitors (CMK, α1-PDX expression in cells) on PC activity in cells and tissues was assessed by the evaluation of the enzymes' ability to digest the universal PC substrate, the fluorogenic peptide pERTKR-MCA, as described previously (8).

Protein extraction and immunoblotting analysis

For total protein extraction, cells were washed with PBS prior to the addition of RIPA lysis buffer. For nuclear fractionation, cells were lysed using a NE-PER nuclear and cytoplasmic extraction reagent kit (Thermo Fisher Scientific) following manufacturer's instructions, and used for Western blot analysis, as described previously (8). Please refer to Supplementary Information for detailed procedures and primary antibodies (Supplementary Table S2).

Cytosolic-free calcium measurement

Jurkat-Ø and PDX cells were loaded with fura-2 by incubation with 4 μmol/L fura-2/AM (Fura-2 acetoxymethyl ester, Molecular Probes) and 2.5 mmol/L probenecid for 30 minutes at 37°C in the dark. Changes in $[Ca^{++}]c$ were monitored using the fura-2 340/380 fluorescence ratio and calibrated according to Grynkiewicz and colleagues (14). Ca^{++} release and entry were estimated using the integral of the rise in $[Ca^{++}]c$ for 3 minutes after the addition of PMA/Io or $CaCl_2$, respectively. In other experiments, Jurkat T cells were incubated with DAPT prior to activation with PMA/Io for Ca^{++} mobilization analysis.

Statistical analysis

Statistical details can be found in Results, Figure, and Figure Legend sections. Data are shown as mean ± SEM or mean ± SD. Analysis of statistical significance was performed using Student *t* test or 1-way ANOVA followed by Bonferroni's comparison as a *post hoc* test. Statistical significance was estimated when $P < 0.05$.

Results

Altered PC expression in human colon cancers, PBMCs, and CD8 T cells

The expression pattern of human PCs namely, furin, PACE4, PC5, and PC7 was analyzed using immunostaining. All of these PCs were expressed in noncancerous colon tissue with the staining particularly localized to the colon crypts (Fig. 1A). In the cancerous tissue from the same patients, we observed alterations of the epithelial structure with the loss of crypts, and an altered expression of all 4 PCs. Only furin showed a highly diffuse expression throughout the tumor. Loss of crypts in colon tissue due to malignant changes is associated with enhanced inflammation and lymphocytic infiltration. Next, we performed real time qPCR to analyze PC expression in human peripheral blood mononuclear cells (hPBMC; Fig. 1B), isolated CD8 T cells (Fig. 1C), Jurkat T cells (Fig. 1D), and other human T-cell lines (Supplementary Fig. S1A). We found that furin and PC7 are the main PCs expressed in all these cells. Similarly, immunofluorescence staining of hPBMCs confirmed the expression of these PCs in CD8 T cells of healthy donors (nontumoral, NT) and patients with colon cancer (tumoral: T; Fig. 1E; Supplementary Fig. S1B–S1C). Further analysis of colon cancer tissue revealed that although various cells within the tumors express furin, a population of tumor infiltrating CD8 T cells expressed furin and PC7 (Fig. 1F). This points to the presence of PCs in tumor-infiltrating lymphocytes (TIL) particularly CD8 T cells, which may have a role in their phenotype and activity.

Published OnlineFirst July 29, 2019; DOI: 10.1158/0008-5472.CAN-19-0086

Inhibition of PCs activity represses PD-1 expression in T cells

Previously, the activity of furin and PC7 in various cells was reported to be significantly inhibited by the general protein-based inhibitor α1-PDX (PDX) and by the pharmacologic inhibitor decanoyl-Arg-Val-Lys-Arg-chloromethylketone (CMK; refs. 7, 8). To investigate the potential role of PC activity on PD-1 expression, we examined the effect of PC inhibition on PD-1 mRNA expression in Jurkat T cells stably expressing the PC inhibitor α1-PDX. In an *in vitro* enzymatic digestion assay (15), using the fluorogenic peptide pERTKR-MCA as PCs substrate, we show that the expression of α1-PDX in these cells (Jurkat-PDX) inhibits PC activity compared with cells expressing empty vector (Jurkat-Ø; Fig. 2A and B). Similarly, the ability of Jurkat-PDX to mediate the cleavage of the PC substrate IGF-I receptor precursor (ProIGF-IR, ∼200 kDa; ref. 8) into its processed form (∼97 kDa) was inhibited (Fig. 2C). T cells require both calcium and protein kinase C (PKC) signal for their activation. PMA binds to and activates PKC whereas ionomycin (Io) is a calcium ionophore that enhances membrane permeability to calcium. Combination of PMA and Io (PMA/Io) mimics T-cell receptor (TCR) activation. We found that in Jurkat-Ø cells PMA/Io induced PD-1 mRNA expression at various time points. In contrast, in Jurkat-PDX cells PD-1 mRNA expression was considerably decreased (Fig. 2D). Flow cytometry (Fig. 2E and F) and immunofluorescence staining (Fig. 2G and H) analyses confirmed that PD-1 protein was greatly decreased in the presence of α1-PDX. These observations indicate that PCs are involved in PD-1 expression and that PC inhibitors can impede PD-1 expression at the RNA and protein levels. Similarly, following anti-CD3–mediated activation revealed that α1-PDX expression led to a significant decrease in PD-1 expression at the RNA (Fig. 2I) and protein levels (Fig. 2J and K). To corroborate these results, hPBMCs from healthy donors were treated with the general convertases pharmacological inhibitor, CMK, for 24 hours prior to anti-CD3–mediated activation. In these cells CMK induced a significant decrease in PD-1 expression, as assessed by flow cytometry gating for lymphocytes (Fig. 2L and M) and immunofluorescence analysis for hPBMCs (Fig. 3A and B; Supplementary Fig. S2A–S2B). CMK inhibition of PC activity was confirmed using the enzymatic digestion assay and immunoblotting (Supplementary Fig. S2C). Immunofluorescence analysis of hPBMCs from colon cancer patients, treated with CMK for 48 hours and CD3-activated showed a 33% reduction of $CD8^{+}/PD\text{-}1^{+}$ cells (Fig. 3C and D). Total PD-1 expression was also significantly reduced in CMK-treated tumoral hPBMCs (Supplementary Fig. S2D). No significant difference was observed in the total number of CD8 cells between conditions, remaining at 25.5% ± 5.7 of total cells (Supplementary Fig. S2E). We next evaluated whether PCs inhibition may also affect the expression of other immune checkpoints. We found that although T-cell activation induced the expression of Tim3, BTLA, LAG3, TIGIT, and CTLA4, PCs inhibition by α1-PDX significantly repressed the expression of TIM3 and BTLA. No evident effect on LAG3, TIGIT, and CTLA4 expression was observed (Fig. 3E).

PCs inhibition represses calcium mobilization and NFAT signaling in T cells

Cytosolic-free calcium concentration ($[Ca^{2+}]_c$) was measured within 3 minutes of PMA/Io stimulation of Jurkat-Ø and Jurkat-PDX cells to detect the effect of PMA/Io-mediated activation on calcium release from intracellular stores. In the absence of extracellular calcium (250 mmol/L EGTA added), intracellular calcium concentration after PMA/Io treatment was lower in Jurkat-PDX cells than in Jurkat-Ø cells, with a 40% less mobilization in Jurkat-PDX cells (Fig. 3F–H). Subsequent addition of 1 mmol/L $CaCl_2$ to the extracellular medium revealed no significant differences in calcium entry in both Jurkat-Ø and Jurkat-PDX cells (Fig. 3I). Calcium signaling upon activation in T cells induces NFAT nuclear translocation necessary for PD-1 expression. We found that total levels of NFAT in nonactivated cells (cytosolic and nuclear) were higher in Jurkat-PDX (Fig. 3J). However, PMA/Io stimulation induced a time-dependent nuclear accumulation of NFAT in Jurkat-Ø cells whereas nuclear NFAT decreases with time in Jurkat-PDX cells (Fig. 3K). These results indicate that PCs blockade inhibits calcium/NFAT signaling necessary for PD-1 expression in T cells.

PCs inhibition represses NF-κB and induces ERK phosphorylation in T cells

We next investigated the effect of PC inhibition on PKC/NF-κB and MAPK/ERK signaling pathways. It was previously shown that PKC/NF-κB signaling is necessary for PD-1 expression in macrophages (16); however, its implication in PD-1 expression in T cells is unclear. NF-κB phosphorylation was clearly reduced when T cells were stimulated with PMA or Io alone (Supplementary Fig. S3A). Accordingly, only PMA/Io activation significantly induced PD-1 expression at the RNA and protein levels (Supplementary Fig. S3B–S3C). Furthermore, PC inhibition blocked NF-κB phosphorylation after PMA/Io stimulation correlating with the effect on PD-1 expression (Fig. 3L). These results suggest that not only calcium but also PKC/NF-κB is involved in PD-1 expression in T cells and the combination of both produces a synergistic effect. Interestingly, incubation of cells with BMS345541, an inhibitor of NF-κB activity (Fig. 3M), partially repressed PD-1 protein expression in PMA/Io-activated cells (Fig. 3N), emphasizing that NF-κB activity is not the only pathway responsible for PD-1 expression in these cells. Analysis of ERK phosphorylation in Jurkat cells revealed that their stimulation by PMA or PMA/Io induced a similar level of phosphorylation whereas Io alone was not able to induce ERK phosphorylation at any of the time points analyzed (Supplementary Fig. S4A). In contrast to NF-κB, ERK phosphorylation induced by PMA/Io was higher in Jurkat-PDX cells than in Jurkat-Ø cells (Fig. 4A), suggesting an ERK-independent mechanism of PC-mediated regulation of PD-1. Taken together, we have shown that PC inhibition affects the activation of different T-cell signaling effectors, principally or partially involved in PD-1 expression.

Increased T-cell survival and proliferation by PC activity blockade

It has been previously reported that exhausted T cells expressing PD-1 exhibit proliferation impairment and progress to apoptosis due to their inability to differentiate into memory T cells (17). We investigated whether PC activity blockade could rescue activated T-cell proliferation and survival. Proliferation was assessed on Jurkat cells for 72 after 3 hours stimulation with PMA/Io. We found that although both Jurkat-Ø and Jurkat-PDX cells show similar proliferative rate in the absence of PMA/Io, the proliferation of Jurkat-Ø cells after adding PMA/Io was inhibited. In contrast, the expression of α1-PDX prevented PMA/Io-driven repression of cell proliferation (Fig. 4B). Furthermore, long-term stimulation of Jurkat-Ø cells with PMA/Io strongly blocked their proliferation. In contrast, although the long-term

Published OnlineFirst July 29, 2019; DOI: 10.1158/0008-5472.CAN-19-0086

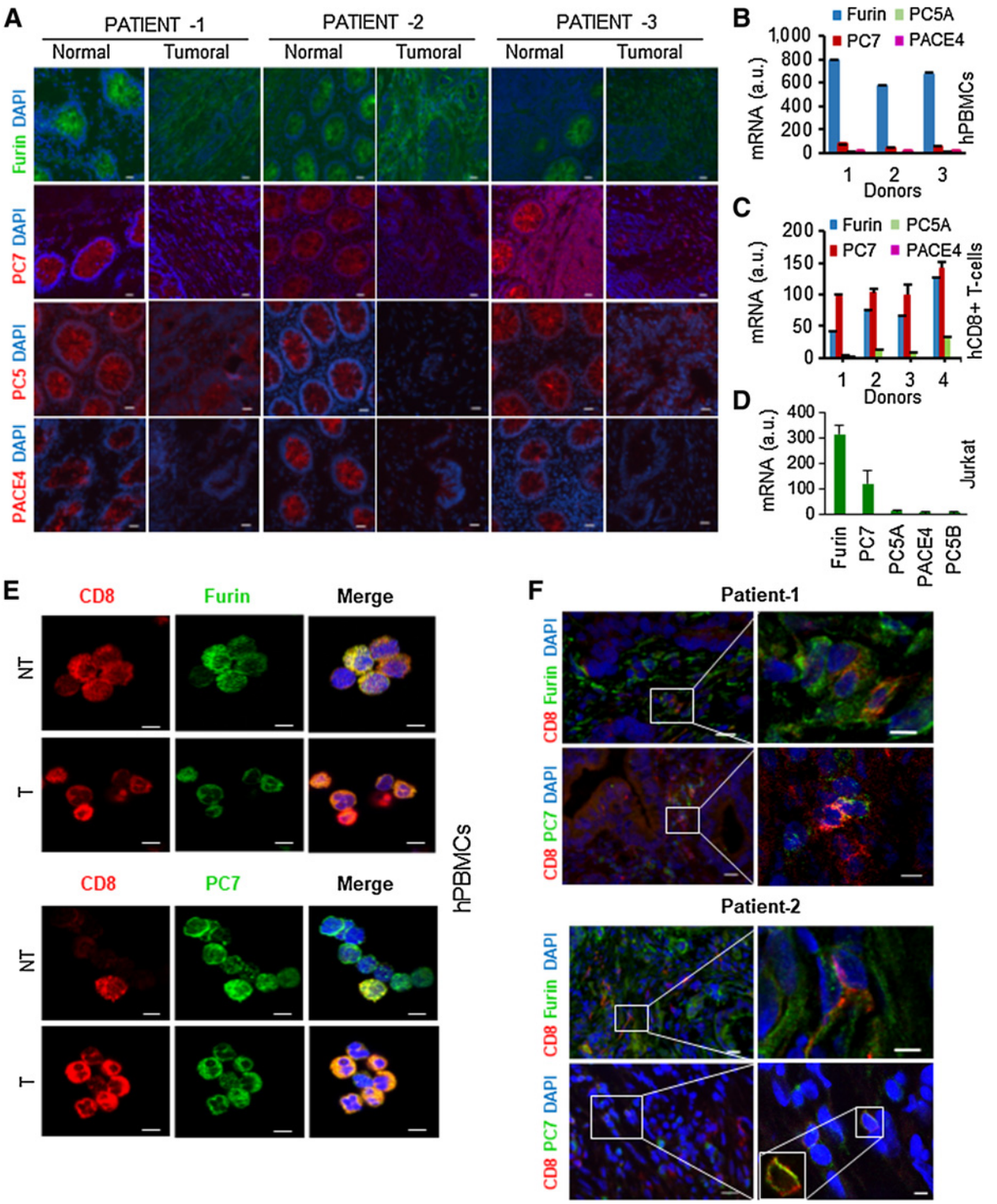

Figure 1.

Altered PC expression in human colon cancer tissues and T cells. **A,** Representative confocal microscopy images of PC immunofluorescence of frozen sections from colon tumors and their adjacent normal tissues of three different patients. Scale bar, 20 μm. **B,** PC mRNA levels in hPBMCs isolated from three different healthy donors determined by qRT-PCR. **C,** qRT-PCR analysis of PCs mRNA levels in human $CD8^+$ T cells isolated by magnetic beads from hPBMCs of four healthy donors. **D,** PC mRNA levels in Jurkat T cells determined by qRT-PCR. **E,** Representative confocal microscopy images of CD8 (red), furin (green), and PC7 (green) immunofluorescence of hPBMCs from healthy donors (NT, nontumoral) and patients with colon cancer (T, tumoral). Scale bar, 5 μm. **F,** Representative confocal microscopy images of CD8 (red), furin (green), or PC7 (green) immunofluorescence of tumoral tissue frozen sections from two different patients with colon cancer. Scale bars, 20 μm for the left image and 5 μm for the right image. Data represented as mean ± SD for each donor (**B** and **C**) or as mean ± SEM from two independent experiments (**D**). a.u., arbitrary units.

Published OnlineFirst July 29, 2019; DOI: 10.1158/0008-5472.CAN-19-0086

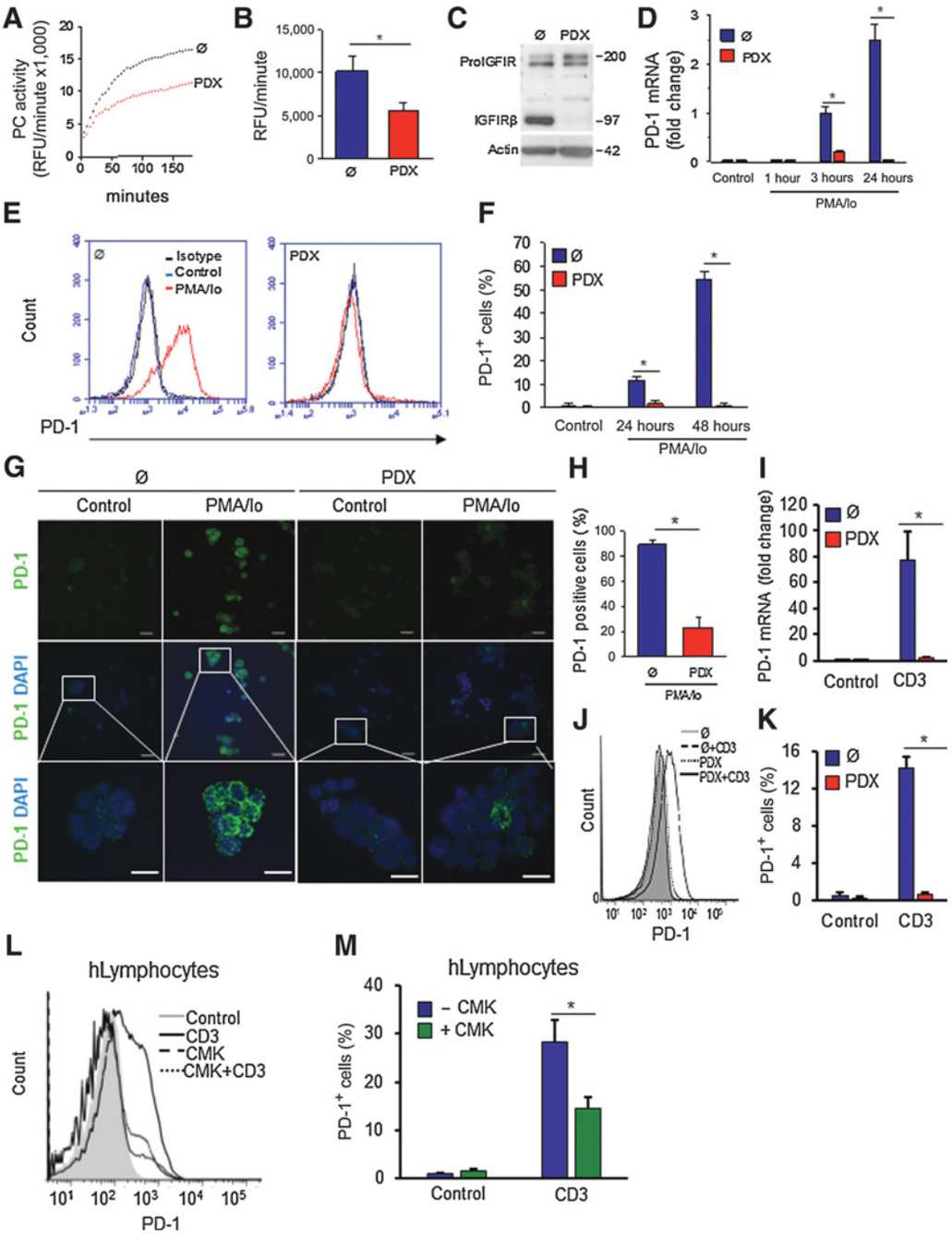

Figure 2.

Inhibition of PC activity represses PD-1 expression in T cells. **A,** Kinetics of PC activity performed in control (∅) and α1-PDX-expressing (PDX) cells. RFU, relative fluorescence unit. **B,** PC activity values at the half of V_{max} in ∅ and PDX cells. **C,** Western blot analysis showing IGF-IR precursor (Pro IGF-IR) and processed (IGF-IRβ) forms in ∅ and PDX cells. **D,** PD-1 mRNA levels upon PMA/Io stimulation at different time points in ∅ and PDX cells assessed by RT-PCR. Data are represented as fold change to 3-hour time point that was assigned 1. **E,** Flow cytometry histogram of PD-1 expression in controls (blue) and 48 hours PMA/Io-stimulated (red) Jurkat-∅ and Jurkat-PDX cells. **F,** Flow cytometry analysis of PD-1 expression at different time points in PMA/Io-stimulated ∅ and PDX cells, shown as the percentage of positive cells. **G,** Representative confocal images of PD-1 immunofluorescence (green) of ∅ and PDX cells in nontreated (Control) and after 48 hours of PMA/Io treatment. Scale bars, 10 and 5 μm. **H,** Immunofluorescence image quantification of PD-1-positive cells (as shown in **G**) relative to total cell number (DAPI) from at least four different images and three different areas per image. **I,** PD-1 mRNA levels in Jurkat-∅ and PDX cells upon anti-CD3–mediated activation represented as the fold change to Jurkat-∅ control. Flow cytometry histogram (**J**) and analysis (**K**) of PD-1 expression in control and anti-CD3–activated Jurkat-∅ and PDX cells. **L,** Flow cytometry histogram of PD-1 expression in human lymphocyte population gated from isolated hPBMCs. CMK was added 24 hours before anti-CD3 activation for 6 hours. **M,** Flow cytometry analysis of PD-1 expression in the cells described in **L**, represented as the percentage of positive cells. Data represented as mean ± SD (**B**) and mean ± SEM from three independent experiments (**D**, **F**, **H**, **I**, **K**, and **M**). *, $P < 0.05$.

Published OnlineFirst July 29, 2019; DOI: 10.1158/0008-5472.CAN-19-0086

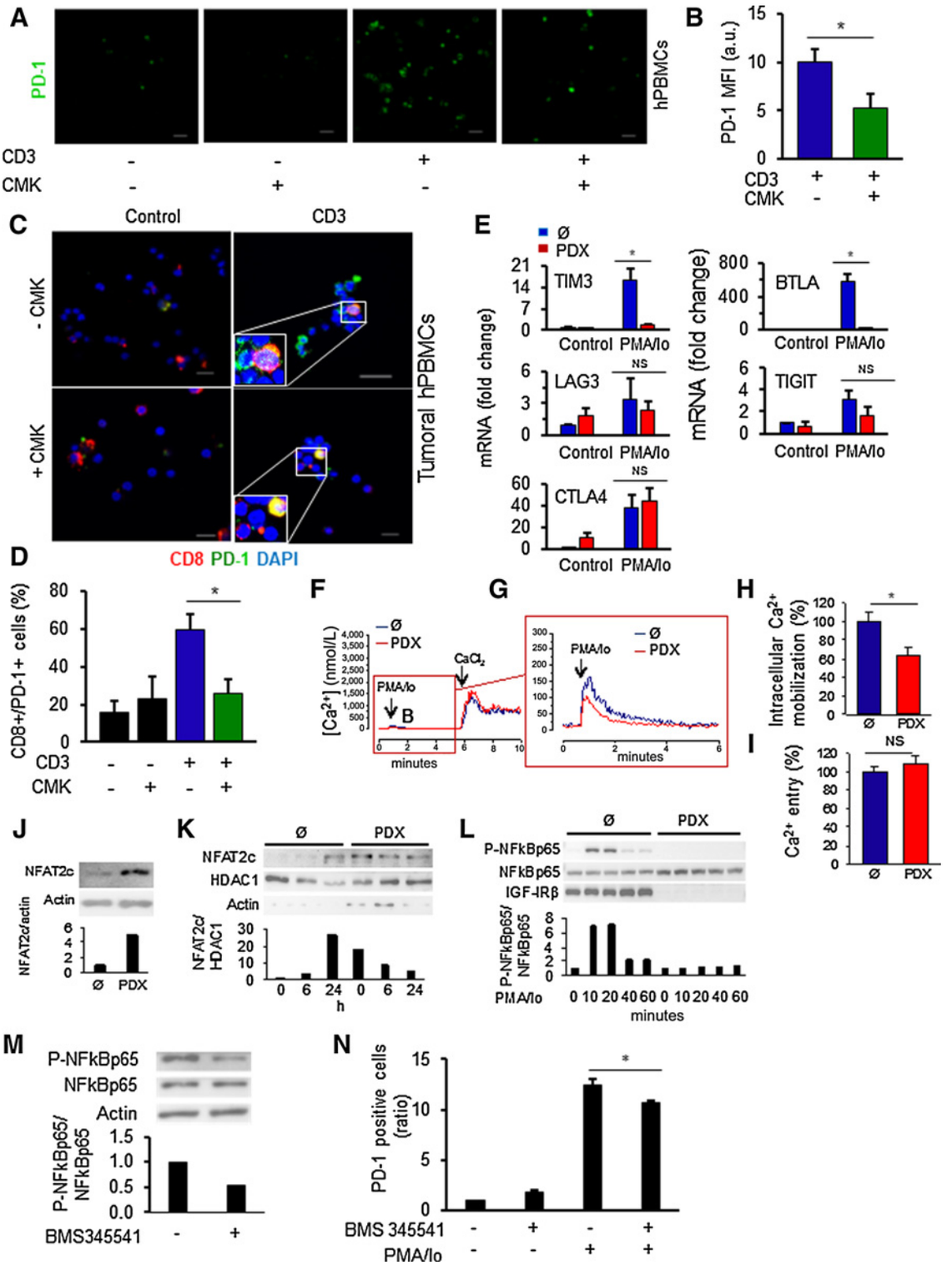

Figure 3.

Inhibition of PCs activity represses PD-1 expression and calcium/NFAT and NF-κB signaling pathways. **A,** Representative confocal microscopy images of PD-1 immunofluorescence (green) of hPBMCs from nontumoral donor. Scale bar, 10 μm. **B,** Immunofluorescence image quantification of PD-1 (as shown in **A**), represented as the mean fluorescence intensity (MFI) from at least four images and three different areas per image. **C,** Representative confocal microscopy images of CD8 (red) and PD-1 (green) immunofluorescence from hPBMCs isolated from patient with colon cancer. (*Continued on the following page.*)

Published OnlineFirst July 29, 2019; DOI: 10.1158/0008-5472.CAN-19-0086

stimulation also reduced Jurkat-PDX cell proliferation, they still showed a higher proliferation rate than Jurkat-Ø cells (Fig. 4B). Because T-cell activation can trigger apoptosis to downregulate T-cell activity, we next analyzed the role of PC inhibition in T-cell activation-mediated apoptosis. Flow cytometry–based detection of Annexin V and 7AAD double-staining showed differences in cell death upon PMA/Io stimulation. In nonstimulated Jurkat-Ø and -PDX cells, the overall percentage of dead cells was very similar (9.1 ± 1.3% and 10.9 ± 0.2, respectively; Fig. 4C; Supplementary Fig. S4B). Upon their activation with PMA/Io, we observed a significant increase in the number of Jurkat-Ø apoptotic cells. In Jurkat-Ø cells, the percentage of dead cells after 48 hours of PMA/Io stimulation was 23.9 ± 2.8% whereas Jurkat-PDX cells showed reduced apoptotic levels with only 7.8 ± 0.7% of dead cells. Similarly, in Jurkat-Ø cells, cleaved caspase-3 was detected after 24 hours of PMA/Io stimulation and further increased following 48 hours of treatment (Fig. 4D). In Jurkat-PDX cells, cleaved caspase-3 was not detected at 24 or 48 hours, confirming the protective effect of the PCs inhibitor in T cells. BCL11B is a survival protein regulated by ERK activation that is essential for T-cell commitment and specification of mature T-cell lineages, including cytotoxic CD8 cells (18). Analysis of BCL11B expression upon PMA/Io stimulation revealed a time-dependent reduction in Jurkat-Ø cells, while its expression was maintained at all time points in Jurkat-PDX cells (Fig. 4D). Downregulation of BIM protein, a member of BH3-only subset of Bcl-2 family, is required for activated T-cell survival (19). We observed high levels of BIM expression in nonactivated Jurkat-Ø and -PDX cells (Fig. 4E), with lower levels (particularly BIM_{EL} and BIM_{L}) in the latter. Stimulation with PMA/Io significantly decreased BIM levels in Jurkat-Ø cells and even more in Jurkat-PDX cells. Interestingly, the higher reduction of BIM in Jurkat-PDX cells correlates with the enhanced ERK phosphorylation we have shown (Fig. 4A), and supporting the prosurvival role of ERK signaling in T cells by inhibiting BIM expression (20).

PC activity inhibition in T-cell cytotoxicity

In addition to high levels of inhibitory receptor expression, T cells have impaired cytotoxicity in cancer (21). Cytotoxic CD8 T cells typically utilize 2 major contact-dependent pathways to kill target cells (22): the granule exocytosis and Fas–Fas ligand (FasL) pathway. Granulysin and perforin mediate the delivery of the apoptosis-inducing proteases, granzymes A and B, into the target cells through the granule exocytosis pathway. The Fas–Fas ligand (FasL) pathway activates caspase-mediated apoptosis. The release of cytotoxic proteins was tested by cytometric bead array in conditioned medium from purified CD8 T cells pretreated with CMK followed by anti-CD3–mediated activation (Fig. 4F). Conditioned medium from control activated CD8 T cells showed high levels of granzyme A and perforin compared with nonactivated cells. CMK alone was able to increase the amount of granzyme A and granulysin, which increased further upon cell activation (Fig. 4F). Similarly, compared with control cells, anti-CD3–mediated activation of CD8 T cells in the absence or presence of CMK causes the release of sFasL (Fig. 4G). Analysis of CD107a expression, a cytotoxic T-cell degranulation marker, showed a similar increase in CD107a positive cells after activation, in both CMK-treated and non-treated hPBCMs (Fig. 4H; Supplementary Fig. S4C). Further analysis of anti-CD3–activated hPBMCs from different donors revealed similar high levels of granzyme B mRNA in the absence and presence of CMK (Fig. 4I). Taken together, these data indicate the preservation of the cytotoxic machinery in the presence of CMK. To further support the effector function of T cells after PC inhibition, a cell-based cytotoxicity assay was performed using hPBMCs and the human colon cancer cells HT29 (MSS) and HCT116 (MSI). As expected, the lysis of HT29 cells was more efficient in activated hPBMCs both in the presence and absence of CMK (Fig. 4J). Moreover, in 2 of the 3 donors, the percentage of lysis was higher with CMK-treated hPBMCs. Similarly, the analysis of caspase-3 from the coculture of anti-CD3–activated hPBMCs treated with CMK with another human colon cancer cell line (HCT116) corroborated the cytotoxicity assay. Caspase-3 cleavage was increased after hPBMC activation, compared with nonactivated cells, with or without CMK (Fig. 4K). These findings indicated the ability of CMK-treated hPBMCs to kill MSI and MSS colon cancer cells. We next analyzed the expression of CD69, a T-cell activation marker, by flow cytometry to test whether the inhibition of PCs in T cells could affect antigen-TCR binding and therefore, downstream T-cell activation. TCR-deficient Jurkat cells (JRT3), expressing a specific TCR (LES) that recognizes the EPCR protein, were coculture with EPCR-expressing HT29 cancer cells. As expected, CD69 expression was upregulated when JRT3-LES cells were cocultured with EPCR-expressing HT29 cells. Similarly, JRT3-LES treated with CMK for 24 hours strongly upregulated CD69 expression in the presence of the cancer cells (Fig. 4L; Supplementary Fig. S4D). Western blot analysis of IGF-IR receptor cleavage confirmed PC activity inhibition by CMK in JRT3-LES cells (Fig. 4M). The survival factor BCL11B was upregulated in JRT3-LES cells after CMK treatment (Fig. 4M), confirming our previous results in Jurkat-PDX cells (Fig. 4D) and highlighting the survival role of CMK during JRT3-LES/cancer cell interaction. Altogether, these findings show that PC blockade repressed PD-1 expression in T cells without affecting their ability to recognize cancer cells and mediate cytotoxicity.

PC inhibition represses tumor growth and increases infiltrated T cells with repressed PD-1

Next, we analyzed whether the effect of PC inhibition that we observed on T cells would translate into a better cancer immunoresponse *in* vivo, with a particular interest in cytotoxic T-cell

(*Continued.*) Scale bar, 10 μm. **D,** Immunofluorescence image quantification of PD-1 and CD8 double-positive hPBCMs from patient with cancer (as shown in **C**) relative to total $CD8^+$ cells (three different images and three different areas per image). **E,** qRT-PCR analysis of TIM3, BTLA, LAG3, TIGIT, and CTLA4 expression in PMA/Io activated Jurkat Ø and PDX cells. **F,** PMA/Io-mediated intracellular calcium mobilization in Jurkat Ø and PDX cells. **G,** Calcium graph section framed in **F** after PMA/Io-induced calcium mobilization from intracellular stores in Ø and PDX cells. **H** and **I,** Bar graphs represent the amount of intracellular calcium mobilization from intracellular stores (**H**) or calcium entry (**I**) in Ø and PDX cells as described in Materials and Methods. **J** and **K,** Western blot and densitometry analyses of NFAT2c levels in whole lysates (**J**) and nuclear fractions (**K**) at different time points after PMA/Io stimulation of Ø and PDX cells. **L,** Western blot and densitometry analyses of P-NFkBp65 at different time points of PMA/Io stimulation in Ø and PDX cells. **M,** Western blot and densitometry analyses of P-NFkBp65 after NF-κB inhibitor BMS345541 treatment. **N,** Flow cytometry analysis of PD-1 expression (% positive cells) in BMS345541-treated Jurkat-Ø cells relative to control condition (nonactivated and without BMS345541). Data represented as the mean ± SEM from three independent experiments.
*, $P < 0.05$.

Published OnlineFirst July 29, 2019; DOI: 10.1158/0008-5472.CAN-19-0086

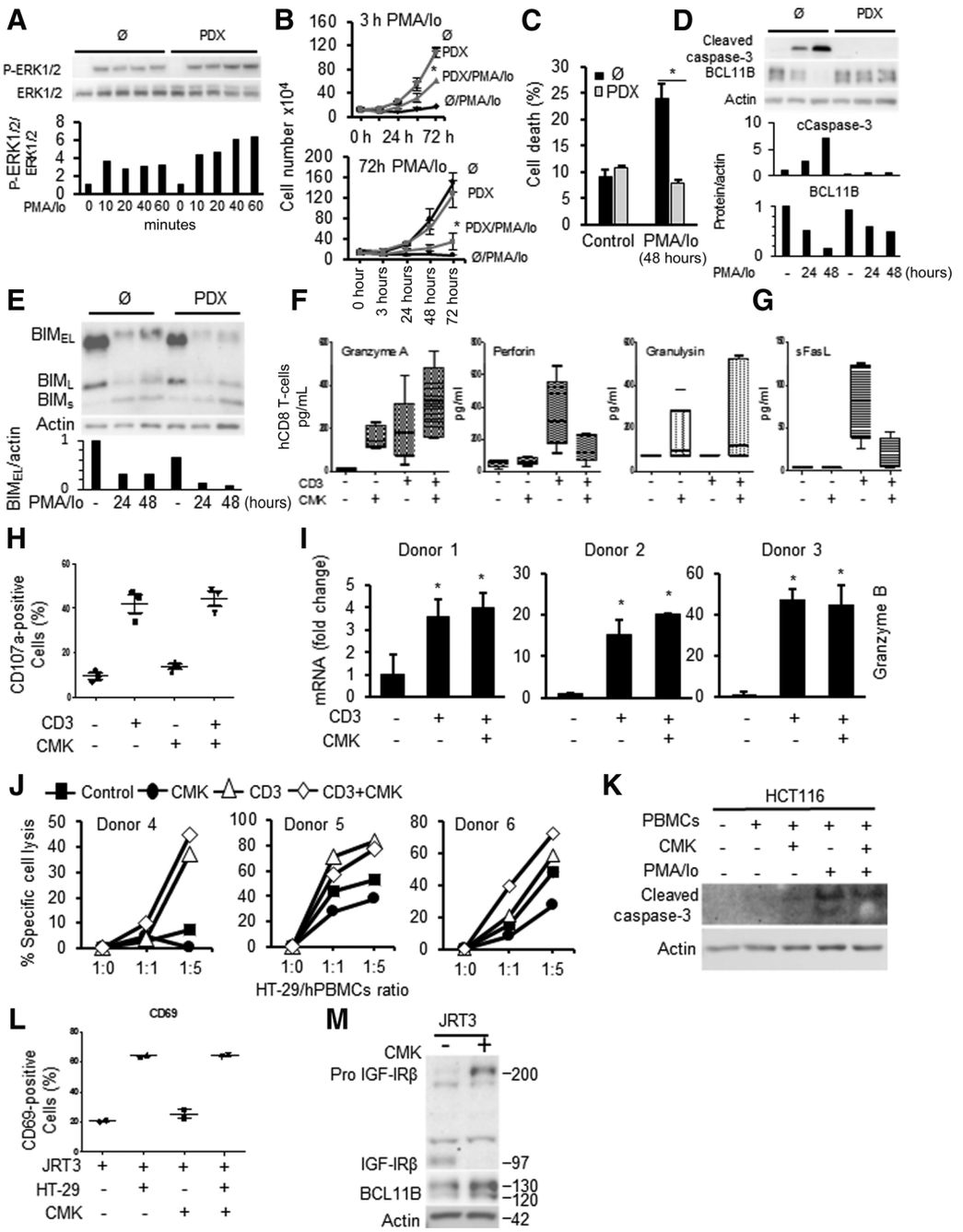

Figure 4.

Increased ERK activation and T-cell proliferation, survival, and cytotoxicity by PC activity blockade. **A,** Western blot and densitometry analyses of P-ERK1/2 at different time points of PMA/Io stimulation of Jurkat-∅ and -PDX cells. **B,** Effect of short (3 hours) and prolonged (72 hours) PMA/Io stimulation on Jurkat-∅ (black) and -PDX (gray) cell proliferation. **C,** Flow cytometry analysis of cell death (% of Annexin-V+/7AAD+) after 48 hours PMA/Io stimulation. **D** and **E,** Western blot and densitometry analyses of cleaved caspase-3 and the prosurvival factor BCL11B (**D**) and BIM (**E**) at 24 and 48 hours of PMA/Io stimulation. **F** and **G,** Levels of cytolytic proteins released by isolated human CD8 T cells measured by a CBA assay. Cells were treated with CMK for 24 hours prior to anti-CD3 activation (6 hours). **H,** Flow cytometry analysis of the cytotoxic-activity marker CD107a in hPBMCs treated with CMK for 24 hours, followed by anti-CD3 for 6 hours from three different donors. **I,** Granzyme B mRNA levels in hPBMCs isolated from three different donors expressed as fold change to control (CD3- and CMK-). **J,** Cytotoxicity flow cytometry-based assay show tumor cell-specific lysis (HT-29 cells) after coculture with hPBMCs treated with CMK. Results from three different donors are shown. **K,** Western blot analysis of cleaved caspase-3 in HCT116 tumor cells after coculture with hPBMCs for 48 hours (target:effector ratio = 1:5). **L,** JRT3 functional assay; flow cytometry analysis of TCR-activation marker CD69 in JRT3 cells upon binding to HT29 cancer cells. **M,** JRT3 cells treated with CMK prior to coculture with HT-29 cells showed reduction in IGF-IR maturation and increased BCL11B expression. Data represented as the mean ± SEM from three independent experiments. *, $P < 0.05$.

Published OnlineFirst July 29, 2019; DOI: 10.1158/0008-5472.CAN-19-0086

infiltration and PD-1 expression. We used the syngeneic murine colon cancer cell line CT26 and the same cells stably expressing α1-PDX (CT-26-PDX) to induce tumors in the immunocompetent BALB/c mice and in nude mice with T-cell deficiency. Because the tumor cells express α1-PDX, we first analyzed the ability of these cells to release α1-PDX in cultured medium and the ability of this conditioned medium to inhibit PC activity in other cells. Thus, we analyzed the processing of 2 PC substrates, namely PDGFA (23) and IGF-IR (8). The conditioned media from CT26 control cells and the same cells cotransfected with cDNAs coding for V5-α1-PDX and V5-proPDGFA were analyzed by immunoblotting (Fig. 5A). Using an anti-V5 antibody, we detected secreted α1-PDX-V5 (50 kDa) and the accumulation of ProPDGFA-V5 (∼24 kDa) in the conditioned medium from CT26-PDX cells. Furthermore, we found an accumulation of proIGF-IR in Jurkat cells cultured with CT26-PDX conditioned medium (Fig. 5B). CT26-PDX conditioned medium was found to also inhibit pERTKR-MCA cleavage (Fig. 5C). A similar result was obtained with protein extracts from Jurkat cells previously cultured with CT26-PDX conditioned medium (Fig. 5D). CT26-Ø and CT26-PDX cells were analyzed for proIGF-IR processing before subcutaneous inoculation of mice to confirm reduced PC activity in CT26-PDX cells (Fig. 5E). Two groups of BALB/c mice ($n = 6$/group/experiment) and 2 groups of nude mice ($n = 6$/group/experiment) were inoculated with tumor cells and tumor volume was measured at various intervals (Fig. 5F). As previously reported (24), CT26 cells injected in nude mice grow faster whereas compared with the syngeneic BALB/c mice (Fig. 5F and G). Although BALB/c and nude mice injected with CT26-PDX cells showed a significant reduction in tumor growth, the antitumorigenic effect of α1-PDX was more potent in the immunocompetent mice (Fig. 5F and G). These results suggest the dual effect of α1-PDX on both tumor cells growth and T-cell activity to reduce tumor progression. To analyze TILs in immunocompetent mice, 3 weeks after engraftment, tumors from each condition ($n = 6$) were pooled together in groups of 3 for tumor dissociation and analysis. Flow cytometry analysis of CD8 immunofluorescence in dissociated tumors showed almost 2-fold increase in $CD8^+$ T cells within CT26-PDX cell-derived tumors (Fig. 5H and I). In contrast, intratumoral PD-1 immunofluorescence decreased in CT26-PDX cells derived tumors compared with CT26-Ø tumors (Fig. 5J and K). Accordingly, analysis of tumor tissue sections stained for CD8 and PD-1 revealed that, in CT26-Ø tumors, PD-1 positive cells and infiltrated CD8 T cells were mainly located at the periphery in low numbers. On the contrary, in CT26-PDX tumors, a number of dispersed CD8 T cells failed to express PD-1 (Fig. 5L). Altogether, these results strongly suggest that α1-PDX secreted by CT26-PDX tumor cells may also act in a paracrine manner to inhibit PD-1 expression and contribute to CD8 T-cell infiltration in the TME.

Notch precursor maturation and PD-1 expression

Notch is a PC substrate reported to be involved in PD-1 expression in T cells (25). Notch is synthesized as a 300 kDa proprotein (ProNotch-1) that requires PC-based cleavage at RK^{1628} and KR^{1633} sites (site S1 in Fig. 6A) to generate an approximately 120 kDa transmembrane form (NTM; ref. 9). The NTM form is cleaved by ADAM17 at site S2 between the residues Ala^{1710} and Val^{1711} to generate the Notch extracellular truncation (NEXT) domain of 115 kDa. Finally, NEXT cleavage by γ-secretase (S3) between R1751 and R1752 sites generates the Notch intracellular domain (NICD) of 110 kDa (Fig. 6A). Immunoblotting analysis of Notch cleavage using an antibody against the NTM domain revealed that whereas both NTM (120 kDa) and ProNotch-1 (300 kDa) forms are observed in control Jurkat cells, ProNotch-1 was the major form observed in Jurkat-PDX cells (Fig. 6B). Incubation of Jurkat-Ø cells with CMK also induced the accumulation of the unprocessed form of Notch (Fig. 6B). Using an antibody against the NICD form (totally processed active form), we found reduced NICD level in Jurkat-PDX compared with Jurkat-Ø cells upon activation (Fig 6C). To test whether both PC and γ-secretase are required to act in a stepwise process to generate NICD prior to PD-1 expression, we first used the γ-secretase inhibitor, DAPT (Fig. 6D–F). PD-1 expression in PMA/Io-activated Jurkat-Ø cells was repressed by DAPT as shown by the reduction in PD-1 mRNA levels (Fig. 6F). Flow cytometry analysis also showed a significant reduction of PD-1 at the protein level after DAPT treatment (Fig. 6F). To further assess the importance of proNotch cleavage in PD-1 expression, NICD was expressed in Jurkat-PDX cells using lentiviral vector containing human NICD cDNA (Fig. 6G). We observed that although the presence of α1-PDX repressed PD-1 expression, the lentiviral-mediated expression of NICD (PDX/lentiNICD) induced PD-1 expression (Fig. 6H). Interestingly, although PD-1 levels were significantly increased compared with nonstimulated Jurkat-Ø and stimulated Jurkat-PDX, the restoration of NICD failed to promote PD-1 expression at the levels observed in activated Jurkat-Ø cells (Fig. 6H). Next, we investigated whether Notch activity affects PD-1 expression through the signaling pathways implicated in T-cell activation/exhaustion. Calcium/NFAT and NF-κB/ERK pathways were analyzed in Jurkat cells after DAPT treatment (Fig. 6I–K). As illustrated in Fig. 6I, the calcium response to PMA/Io treatment was inhibited by DAPT. Similarly, nuclear accumulation of NFAT following PMA/Io stimulation was reduced in DAPT-treated cells, as assessed by Western blot analysis (Fig. 6J) and by EGFP-based reporter assay containing an NFAT-sensitive promoter (Fig. 6K). Treatment with DAPT had no effect on NF-κB and ERK phosphorylations upon PMA/Io stimulation (Fig. 6J). These findings indicate that although Notch cleavage is required for calcium mobilization and NFAT activation, pathways involved in PD-1 expression, mature Notch is not able to completely rescue PD-1 expression in PC-inactivated cells. The results suggest that there might be other PC substrates, unprocessed/inactivated by PC inhibitors, involved in the regulation of PD-1 expression through calcium/NFAT, NF-κB, and probably other signaling pathways. Altogether, we propose a mechanism of action in which PC inhibition disrupts PD-1 expression in T cells through Notch processing blockade (and probably other precursors) and calcium/NFAT and NF-κB pathway inhibitions. In consequence, the reduced expression of PD-1 receptor at the cellular membrane of T cells, allows T cells to bypass the PD-L1/PD-1 mechanism developed by cancer cells to avoid the immune response.

Discussion

In cancer, T cells are chronically exposed to persistent antigen stimulation. This is often associated with deterioration of T-cell function and inefficient control of tumors. Immune checkpoint blockade can reinvigorate dysfunctional/exhausted T cells by restoring immunity to eliminate cancer cells. In this study, we identified PCs as new key players in the regulation of the PD-1 expression and cytotoxicity against tumor cells.

Published OnlineFirst July 29, 2019; DOI: 10.1158/0008-5472.CAN-19-0086

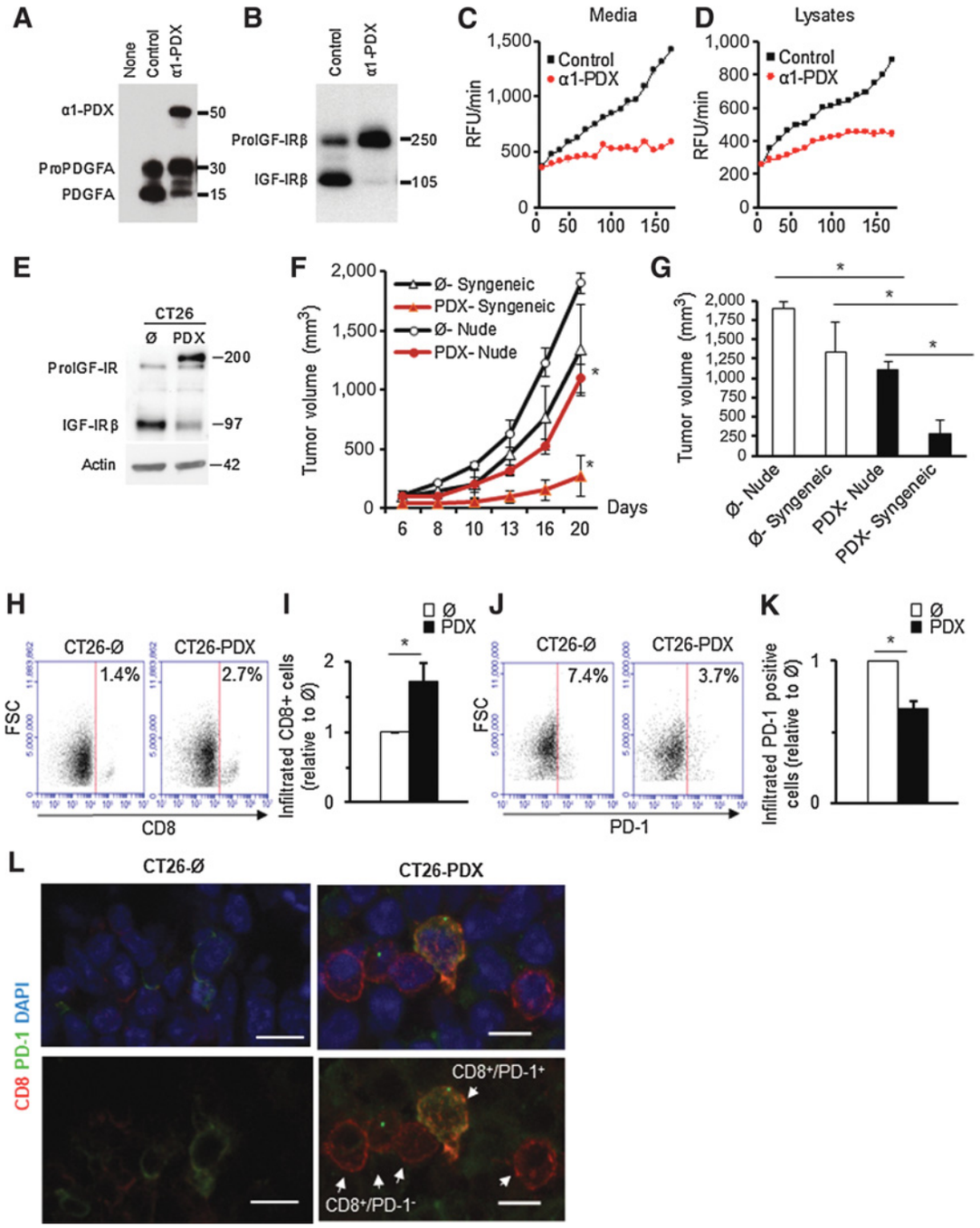

Figure 5.

PC inhibition represses tumor growth and increases TILs. **A,** Western blot analysis showing the precursor and processed forms of the PC substrate PDGFA and α1-PDX, accumulated in conditioned medium of control or α1-PDX-expressing CT26 cancer cells. **B,** Western blot analysis for IGF-IR from Jurkat cells previously treated with CT26 and CT-26/PDX conditioned medium. **C** and **D,** Kinetics of PC activity performed on conditioned media from control and α1-PDX-CT26 cells (**C**) and on Jurkat cells cultured in those conditioned media (**D**). **E,** Western blot analysis showing IGF-IR processing in CT26-Ø and CT26-PDX cells prior to mouse inoculation. **F,** Tumor growth analysis of subcutaneously injected CT26-Ø and CT26-PDX cells in syngeneic immunocompetent BALB/c mice and nude mice. **G,** Comparative analysis of tumor growth in the end of the experiment of CT26-Ø and CT26-PDX cells injected syngeneic and nude mice. **H,** Flow cytometry dot plots comparing CD8 expression within CT26-Ø–derived and CT26-PDX–derived tumors. **I,** Flow cytometry analysis of infiltrated $CD8^+$ cells in CT26-Ø–derived and CT26-PDX–derived tumors, represented as relative value to CT26-Ø. **J** and **K,** Flow cytometry dot plots (**J**) and analysis (**K**) of PD-1 in CT26-Ø- and CT26-PDX-derived tumors. **L,** Confocal microscopy images of CD8 (red) and PD-1 (green) immunofluorescence of frozen sections from CT26-Ø–derived and CT26-PDX–derived tumors. Scale bar, 5 μm. Data represented as the mean ± SD (**F**) from 6 mice per condition/experiment. Flow cytometry data (**I** and **K**) obtained from two pools of three tumors each per condition (Ø, PDX) represented as the mean ± SEM. *, $P < 0.05$.

Published OnlineFirst July 29, 2019; DOI: 10.1158/0008-5472.CAN-19-0086

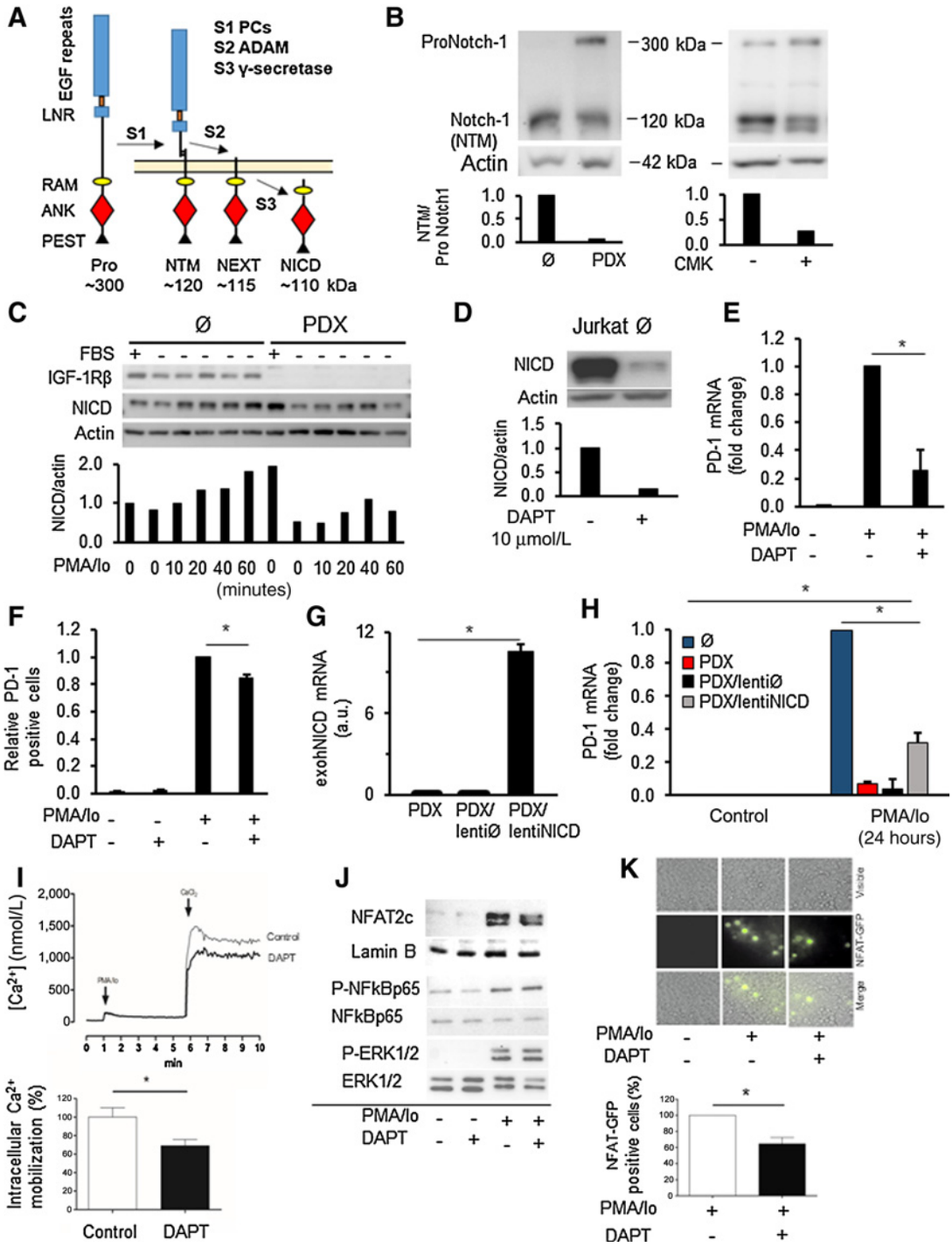

Figure 6.

Notch receptor processing by PCs and PD-1 expression. **A,** Schematic representation of Notch receptor and cleavage sequence. **B,** Western blot and densitometry analyses of Notch-1 processing by PCs in Jurkat Ø and PDX cells, or Jurkat Ø treated with CMK, using an antibody against the transmembrane region (NTM). **C,** Western blot and densitometry analyses of NICD expression upon PMA/Io stimulation of Ø and PDX cells using a NICD-specific antibody. **D,** Inhibition of NICD expression in Jurkat Ø by γ-secretase inhibitor DAPT (10 μmol/L) as shown by Western blot and densitometry analyses. **E** and **F,** PD-1 mRNA (**E**) and protein (**F**) levels in Jurkat-Ø treated with DAPT for 24 hours by qRT-PCR and flow cytometry. **G,** qRT-PCR for NICD mRNA using specific primers for the cloned NICD (exohNICD) to confirm lentiNICD infection in Jurkat-PDX cells. **H,** PD-1 mRNA levels in lentiØ-infected and lentiNICD-infected Jurkat-PDX cells after PMA/Io stimulation. **I–K,** Effect of DAPT on calcium mobilization (**I**), NFAT (**J** and **K**), NF-κB, and ERK (**J**) activation in PMA/Io-activated T cells. Data represented as the mean ± SEM from three independent experiments (**E**, **F**, **I**, and **K**) and mean ± SD (**G** and **H**). *, $P < 0.05$. a.u., arbitrary units.

Published OnlineFirst July 29, 2019; DOI: 10.1158/0008-5472.CAN-19-0086

Most T cells in the TME differentiate into exhausted T cells, express high levels of inhibitory receptors, produce less effector cytokines, and lose the ability to eliminate tumor cells. The final stage of T-cell exhaustion is the physical deletion, by which, severely exhausted T cells are cleared in the TME. Furthermore, T-cell exhaustion may also be related to defective formation of memory T cells. Previously, PD-1 was shown to be overexpressed on tumor-infiltrating $CD8^+$ T cells in multiple solid tumors. Indeed, PD-1^+ $CD8^+$ T cells exhibit an exhausted phenotype characterized by impaired proliferation, cytokine production, and cytotoxicity. Our findings reveal that PC inhibition in activated T cells represses PD-1 expression and enhances TILs. Analysis of several checkpoint proteins revealed that inhibition of the PCs in activated T cells repressed the expression of TIM3 and BTLA and had no effect on LAG3, TIGIT, and CTLA4. T-cell exhaustion is generally characterized by the stepwise and progressive loss of T-cell functions (26, 27), however, other studies revealed that T cells can also be exhausted within hours following virus infection (28). In our studies, we used multiple approaches, including T cell lines, PBMCs, and T cells from healthy and patients with colon cancer as well as a syngeneic mouse tumor model, to study the role of the PCs in PD-1 expression and the signaling pathways involved in PD-1 repression by PCs inhibition. We have shown that furin and PC7 are the main PC family members expressed in T cells, and therefore we have used the general PC inhibitors α1-PDX and CMK known to efficiently repress the activity of both PCs (29, 30). We have shown that PC inhibitors impede PD-1 expression in activated hPBMCs and T cells, and promote proliferation and survival. Our studies also showed that PC inhibitors block PD-1 expression through the repression of both calcium/NFAT and NF-κB activities. An intriguing observation of our signaling analysis was the elevated ERK phosphorylation in activated T cells in the presence of PC inhibitors. The critical role of ERK activation in cell proliferation and survival is well established. ERK activation is necessary for cell-cycle entry as well as cell-cycle checkpoint passage. In addition to proliferation, ERK activation impacts cellular apoptosis. Particularly in T cells, activation of ERK has been shown to inhibit Fas-mediated apoptosis. In accordance with this, the increased proliferation and survival we observed in T cells treated with PC inhibitors could be partially explained by the increased ERK phosphorylation. The molecular mechanism involved in ERK activation by PC inhibition in T cells is currently unknown.

Blocking PD-1/PD-L1 pathway using anti-PD-1 or -PD-L1 monoclonal antibodies is emerging as an effective method for reversing cancer immunosuppression and thereby causing tumor regression in patients with advanced disease. Such treatments have shown promising clinical results not only for tumors classically considered to be immunogenic such as melanoma and renal cell carcinoma, but also for common epithelial malignancies such as non–small cell lung cancer, which is considered to be nonimmunogenic and poorly responsive to immune-based therapies (31, 32). However, in the same clinical trials, no objective responses were observed in patients with colorectal cancers except in a subset of MSI patients (3). The reason for the differential therapeutic effects of targeting PD-1/PD-L1 pathway between colorectal cancers and other cancers is not known. It was reported that the presence of TILs in primary colorectal cancer predicts an improved clinical outcome (33, 34). A high density of infiltrating memory and effector memory T cells within colorectal cancers was associated with decreased invasiveness, lower stage, and improved survival. T cell density in colorectal cancers was found to have stronger prognostic significance than conventional tumor–node–metastasis staging (35, 36). Our study provides clear evidence that antitumor T-cell responses play an important role in determining the clinical outcome for colorectal cancer. We demonstrate that the inoculation of CT26-PDX cells in syngeneic mice induced a better immune response, including increased T cell tumor infiltration and reduced intratumoral PD-1 expression. Importantly, the significant tumor growth repression observed in the syngeneic mice compared with the nude mice, inoculated both with CT26-PDX cells, clearly support the considerable role of PCs inhibition in enhancing tumor immunoresponse. Thus, α1-PDX secreted by the tumor cells represses their survival and growth in addition to playing a paracrine role on activated T by inhibiting PD-1 expression and promoting cytotoxicity. The dual function of α1-PDX on the 2 types of cells within the tumor mass may contribute to a rapid inhibition of tumor development as we observed in the syngeneic model. Thereby, the use of PC inhibitors at the clinical sitting may participate in the efficacy and tolerance of PD-1 immunotherapy in patients with refractory colorectal cancer by combining PC inhibition and reduced practices of immunotherapy treatment. This strategy is feasible since targeting furin by shRNAi DNA combined with GMCSF-secreting autologous immune vaccines was found to be beneficial in patients with advanced cancer (11). Although the restoration of active NICD in α1-PDX–expressing T cells recovered the expression of PD-1, NICD failed to completely restore PD-1. Further investigations are necessary to reveal other PC substrates participating in PD-1 expression.

In summary, we demonstrated a novel interchange between PC activity and PD-1 expression. This regulatory event is critical for T cells to mediate immune surveillance. Importantly, inhibition of PCs in tumor cells promotes tumor-infiltrating cytotoxic T-cell response that coincides with reduced tumor growth. Accordingly, previous studies using different mouse tumor models revealed that T-cell activity and subsequently the status of the antitumor immune response can be influenced by external parameters including the control of the thermoregulation of mice (24), suggesting that the activity of T cells can be modulated by exogenous parameters. Thus, targeting PCs in T cells provides a novel strategy to combat T-cell exhaustion-mediated immunosuppression and may potentially apply to various cancer types.

Disclosure of Potential Conflicts of Interest

No potential conflicts of interest were disclosed.

Authors' Contributions

Conception and design: M. Tomé, G. Siegfried, S. Evrard, A.-M. Khatib

Development of methodology: M. Tomé, A. Pappalardo, F. Soulet, J. Olaizola, Y. Leger, J.A. Rosado, S. Evrard, A.-M. Khatib

Acquisition of data (provided animals, acquired and managed patients, provided facilities, etc.): M. Tomé, F. Soulet, J.J. López, Y. Leger, M. Dubreuil, A. Mouchard, D. Fessart, F. Delom, V. Pitard, D. Bechade, M. Fonck, J.A. Rosado, F. Ghiringhelli, J. Déchanet-Merville, I. Soubeyran, S. Evrard, A.-M. Khatib

Analysis and interpretation of data (e.g., statistical analysis, biostatistics, computational analysis): M. Tomé, F. Soulet, J.J. López, M. Dubreuil, A. Mouchard, D. Fessart, F. Delom, M. Fonck, J.A. Rosado, J. Déchanet-Merville, S. Evrard, A.-M. Khatib

Writing, review, and/or revision of the manuscript: M. Tomé, F. Soulet, J.J. López, J.A. Rosado, F. Ghiringhelli, G. Siegfried, S. Evrard, A.-M. Khatib

Administrative, technical, or material support (i.e., reporting or organizing data, constructing databases): Y. Leger, M. Dubreuil, S. Evrard, A.-M. Khatib
Study supervision: M. Tomé, G. Siegfried, S. Evrard, A.-M. Khatib

Acknowledgments

We thank Juan José Gordillo González de Miranda (Immunology Unit, Department of Physiology, University of Extremadura) for technical assistance. We thank Raúl V. Durán from IECB (Pessac, France) for providing the NICD plasmid, Vect'UB facilities for lentiviral vector production and R. Nookala (Institut Bergonié, Bordeaux, France) for reading the manuscript. This work was supported in part by SIRIC BRIO and La Ligue Contre le Cancer to A.M. Khatib and by MINECO (Grant No. BFU2016-74932-C2), and Junta de Extremadura-FEDER (IB16046) to J.A. Rosado. A.M. Khatib and M. Tomé were supported by the Region Nouvelle Aquitaine and SIRIC BRIO.

The costs of publication of this article were defrayed in part by the payment of page charges. This article must therefore be hereby marked *advertisement* in accordance with 18 U.S.C. Section 1734 solely to indicate this fact.

Received January 8, 2019; revised May 27, 2019; accepted July 22, 2019; published first July 29, 2019.

References

1. Riley JL. PD-1 signaling in primary T cells. Immunol Rev 2009;229:114–25.
2. Ansell SM, Lesokhin AM, Borrello I, Halwani A, Scott EC, Gutierrez M, et al. PD-1 blockade with nivolumab in relapsed or refractory Hodgkin's lymphoma. N Engl J Med 2015;372:311–9.
3. Xiao Y, Freeman GJ. The microsatellite instable subset of colorectal cancer is a particularly good candidate for checkpoint blockade immunotherapy. Cancer Discov 2015;5:16–8.
4. Fearon DT. The carcinoma-associated fibroblast expressing fibroblast activation protein and escape from immune surveillance. Cancer Immunol Res 2014;2:187–93.
5. Joyce JA, Fearon DT. T cell exclusion, immune privilege, and the tumor microenvironment. Science 2015;348:74–80.
6. Sharpe AH, Pauken KE. The diverse functions of the PD1 inhibitory pathway. Nat Rev Immunol 2018;18:153–67.
7. Scamuffa N. Proprotein convertases: lessons from knockouts. FASEB J 2006;20:1954–63.
8. Scamuffa N, Siegfried G, Bontemps Y, Ma L, Basak A, Cherel G, et al. Selective inhibition of proprotein convertases represses the metastatic potential of human colorectal tumor cells. J Clin Invest 2008;118:352–63.
9. Logeat F, Israel A, Seidah NG, Jarriault S, LeBail O, Brou C, et al. The Notch1 receptor is cleaved constitutively by a furin-like convertase. Proc Natl Acad Sci U S A 1998;95:8108–12.
10. Lapierre M, Siegfried G, Scamuffa N, Bontemps Y, Calvo F, Seidah NG, et al. Opposing function of the proprotein convertases furin and PACE4 on breast cancer cells' malignant phenotypes: Role of tissue inhibitors of metalloproteinase-1. Cancer Res 2007;67:9030–4.
11. Senzer N, Barve M, Kuhn J, Melnyk A, Beitsch P, Lazar M, et al. Phase i trial of bi-shRNAi furin/GMCSF DNA/autologous tumor cell vaccine (FANG) in advanced cancer. Mol Ther 2012;20:679–86.
12. Khatib AM, Siegfried G, Prat A, Luis J, Chrétien M, Metrakos P, et al. Inhibition of proprotein convertases is associated with loss of growth and tumorigenicity of HT-29 human colon carcinoma cells: Importance of insulin-like growth factor-1 (IGF-1) receptor processing in IGF-1-mediated functions. J Biol Chem 2001;276:30686–93.
13. Willcox CR, Pitard V, Netzer S, Couzi L, Salim M, Silberzahn T, et al. Cytomegalovirus and tumor stress surveillance by binding of a human γδ T cell antigen receptor to endothelial protein C receptor. Nat Immunol 2012;13:872–9.
14. Grynkiewicz G, Poenie M, Tsien RY. A new generation of Ca2+indicators with greatly improved fluorescence properties. J Biol Chem 1985;260:3440–50.
15. Ma J, Evrard S, Badiola I, Siegfried G, Khatib AM. Regulation of the proprotein convertases expression and activity during regenerative angiogenesis: role of hypoxia-inducible factor (HIF). Eur J Cell Biol 2017;96:457–68.
16. Bally APR, Lu P, Tang Y, Austin JW, Scharer CD, Ahmed R, et al. NF-κB regulates PD-1 expression in macrophages. J Immunol 2015;194:4545–54.
17. Yi JS, Cox MA, Zajac AJ. T-cell exhaustion: characteristics, causes and conversion. Immunology 2010;129:474–81.
18. Wakabayashi Y, Watanabe H, Inoue J, Takeda N, Sakata J, Mishima Y, et al. Bcl11b is required for differentiation and survival of alphabeta T lymphocytes. Nat Immunol 2003;4:533–9.
19. Bouillet P, Metcalf D, Huang DCS. Proapoptotic Bcl-2 relative Bim required for certain apoptotic responses, leukocyte homeostasis, and to preclude autoimmunity. Science 1999;286:1735–8.
20. Korfi K, Smith M, Swan J, Somervaille TCP, Dhomen N, Marais R. BIM mediates synergistic killing of B-cell acute lymphoblastic leukemia cells by BCL-2 and MEK inhibitors. Cell Death Dis 2016;7.
21. Wherry E. T cell exhaustion. Nat Immunol 2011;12:492–9.
22. Russell J, Ley T. Lymphocyte-mediated cytotoxicity. Annu Rev Immunol 2002;20:323–70.
23. Siegfried G, Khatib AM, Benjannet S, Chrétien M, Seidah NG. The proteolytic processing of pro-platelet-derived growth factor-a at RRKR86by members of the proprotein convertase family is functionally correlated to platelet-derived growth factor-A-induced functions and tumorigenicity. Cancer Res 2003;63:1458–63.
24. Kokolus KM, Capitano ML, Lee CT, Eng JWL, Waight JD, Hylander BL, et al. Baseline tumor growth and immune control in laboratory mice are significantly influenced by subthermoneutral housing temperature. Proc Natl Acad Sci 2013;110:20176–81.
25. Mathieu M, Cotta-Grand N, Daudelin JF, Thébault P, Labrecque N. Notch signaling regulates PD-1 expression during CD8+ T-cell activation. Immunol Cell Biol 2013;91:82–8.
26. Wherry EJ, Kurachi M. Molecular and cellular insights into T cell exhaustion. Nat Rev Immunol 2015;15:486–99.
27. Pauken KE, Wherry EJ. Overcoming T cell exhaustion in infection and cancer. Trends Immunol 2015;36:265–76.
28. Hosking MP, Flynn CT, Botten J, Whitton JL. CD8+ memory T cells appear exhausted within hours of acute virus infection. J Immunol 2013;191:4211–22.
29. Lahlil R, Calvo F, Khatib AM. The potential anti-tumorigenic and anti-metastatic side of the proprotein convertases inhibitors. Recent Pat Anticancer Drug Discov 2008;4:83–91.
30. Bontemps Y, Scamuffa N, Calvo F, Khatib AM. Potential opportunity in the development of new therapeutic agents based on endogenous and exogenous inhibitors of the proprotein convertases. Med Res Rev 2007;27:631–48.
31. Brahmer JR, Tykodi SS, Chow LQM, Hwu WJ, Topalian SL, Hwu P, et al. Safety and activity of anti–PD-L1 antibody in patients with advanced cancer. N Engl J Med 2012;366:2455–65.
32. Topalian SL, Hodi FS, Brahmer JR, Gettinger SN, Smith DC, McDermott DF, et al. Safety, activity, and immune correlates of anti-PD-1 antibody in cancer. N Engl J Med 2012;366:2443–54.
33. Ropponen KM, Eskelinen MJ, Lipponen PK, Alhava E, Kosma VM. Prognostic value of tumour-infiltrating lymphocytes (TILs) in colorectal cancer. J Pathol 1997;182:318–24.
34. Naito Y, Saito K, Shiiba K, Ohuchi A, Saigenji K, Nagura H, et al. CD8+ T cells infiltrated within cancer cell nests as a prognostic factor in human colorectal cancer. Cancer Res 1998;58:3491–4.
35. Galon J, Costes A, Sanchez-Cabo F, Kirilovsky A, Mlecnik B, Lagorce-Pages C, et al. Type, density, and location of immune cells within human colorectal tumors predict clinical outcome. Science 2006;313:1960–4.
36. Pagès F, Berger A, Camus M, Sanchez-Cabo F, Costes A, Molidor R, et al. Effector memory T cells, early metastasis, and survival in colorectal cancer. N Engl J Med 2005;353:2654–66.

Published OnlineFirst July 29, 2019; DOI: 10.1158/0008-5472.CAN-19-0086

Cancer Research
The Journal of Cancer Research (1916–1930) | The American Journal of Cancer (1931–1940)

AACR American Association for Cancer Research

Inactivation of Proprotein Convertases in T Cells Inhibits PD-1 Expression and Creates a Favorable Immune Microenvironment in Colorectal Cancer

Mercedes Tomé, Angela Pappalardo, Fabienne Soulet, et al.

Cancer Res 2019;79:5008-5021. Published OnlineFirst July 29, 2019.